ELSEVIER

International Journal of Mass Spectrometry 201 (2000) 297–305

International Journal of Mass Spectrometry

Structural and electronic characterisation of the organometallic distonic ion $(C_6H_6)Fe^+(p\text{-}C_6H_4)^{\cdot}$

Brian F. Yates

School of Chemistry, University of Tasmania, GPO Box 252-75, Hobart TAS 7001, Australia

Received 18 November 1999; accepted 15 February 2000

Abstract

Molecular orbital calculations have been used to characterise the structural and electronic properties of the gas-phase distonic radical cation (benzene)Fe^+(*p*-benzyne)$^{\cdot}$. Geometries and vibrational frequencies were obtained with density functional theory (B3LYP) and additional relative energies calculated with the BLYP, restricted open-shell second order Møller-Plesset (MP2) and spin-projected unrestricted MP2 methods. Doublet, quartet, and sextet spin states were considered. As well as the highly symmetric C_{2v} species, a number of structures with lower symmetry were considered. The radical and charge sites are indeed shown to be separated. Complexation energies of benzene with Fe^+(*p*-benzyne)$^{\cdot}$ were calculated and compared with experimental findings. Calculations on (benzene)Fe(*o*-benzyne)$^{+\cdot}$ and (benzene)Fe(phenyl)$^{+\cdot}$ were also carried out for comparison of structures, electronic properties, and energetics. (Int J Mass Spectrom 201 (2000) 297–305) © 2000 Elsevier Science B.V.

Keywords: Distonic; organometallic; density functional theory

1. Introduction

Fifteen years ago we introduced the term "distonic" radical cation to describe those types of stable radical cations in which the charge and radical sites are separated [1–3]. The concept was generalised by Hammerum to a range of species observable in mass spectrometric experiments [4] and the ion–molecule reactions of distonic radical cations have been reviewed [5]. The term distonic has since been applied to distonic radical anions [6–12], distonic biradical anions [13], distonic biradical cations [14], and distonic carbene ions [15]. A few years ago, the first organometallic distonic radical cation, Fe^+(*p*-benzyne)$^{\cdot}$, was reported [16]. Very recently, the experimental production of a new gas-phase organometallic distonic radical cation (**1**) was described [17] in which the charged site of Fe^+(*p*-benzyne)$^{\cdot}$ has been "covered" with a benzene molecule.

Structure **1** was produced in a Fourier transform ion cyclotron resonance mass spectrometer through a condensation reaction of benzene with Fe^+(*p*-benzyne)$^{\cdot}$. Collision-induced dissociation of **1** was investigated, as well as its reactions with a number of compounds known [5,18,19] to probe the distonic nature of radical cations. It was found that the reactions of structure **1** were quite different to those of the *o*-benzyne isomer, (benzene)Fe(*o*-benzyne)$^{+\cdot}$ (**2**), and its phenyl analogue, (benzene)Fe(phenyl)$^{+\cdot}$ (**3**). In addition, the radical site in **1** appeared to be more

E-mail: Brian.Yates@utas.edu.au (Brian F. Yates)

PII S1387-3806(00)00227-X

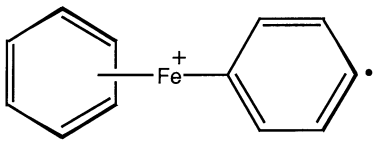

1

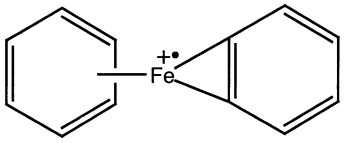

2

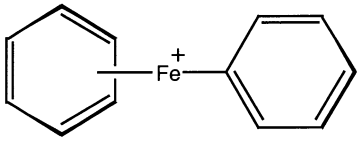

3

Scheme 1.

reactive than in Fe^{+}(*p*-benzyne)$^{\cdot}$, suggesting that the attachment of the benzene molecule enhances the reactivity of the radical site.

In this article we report molecular orbital calculations on structures **1**, **2**, and **3** (corresponding to I, II, and III in the article by Xu et al. [17]) in order to support the rationalisation of the different reactivities of these compounds. We have investigated geometrical structures and the nature of the charge and radical sites in these species.

2. Methods

Full geometry optimisations for systems **1**–**3** and the corresponding fragments [Fe^{+}(*p*-benzyne)$^{\cdot}$, Fe(*o*-benzyne)$^{+\cdot}$, Fe(phenyl)$^{+\cdot}$, and benzene] were carried out with the use of the B3LYP [20–22] density functional level of theory and the LANL2DZ:6-31G(*d*) basis set, which incorporates the Hay and Wadt [23] small-core effective core potential and double-zeta valence basis set on iron, and 6-31G(*d*) [24,25] on the other atoms. Sets of five *d* functions were used in the basis sets throughout these calculations. Several spin states were investigated for each species. In most cases it was difficult to obtain the ground-state wave function straight away, however a judicious use of stability tests [26,27] followed by reoptimisation of the wave function [the "stable = (opt, ruhf)" keyword was used in the GAUSSIAN program] ensured that the appropriate wave function was employed. As expected for these sorts of systems, self-consistent field (SCF) convergence was also a problem in many cases and the use of the quadratically convergent [28] SCF method was required in some situations. For the optimised geometries, harmonic vibrational frequencies were calculated at the B3LYP level and zero-point vibrational energy corrections obtained using unscaled frequencies. Single-point energies were calculated with the BLYP [29–31], ROMP2 [32–35], and PUMP2 [36] methods. All calculations were carried out with the GAUSSIAN 94 [37] and GAUSSIAN 98 [38] programs.

3. Results and discussion

3.1. Electronic states

Total energies for the different spin states of the species studied in this work are shown in Table 1. It can be seen that there is significant spin contamination for some of the species (the $\langle S^2 \rangle$ value for pure doublet, quartet and sextet states is 0.75, 3.75, and 8.75 respectively, while that for pure singlet, triplet, and quintet states is 0, 2, and 6, respectively). Relative energies of these spin states are shown in Table 2 and Fig. 1. Structures **1** and **2** have quartet ground states, while structure **3** has a quintet ground state. For the fragments, Fe^{+}(*p*-benzyne)$^{\cdot}$ and Fe(*o*-benzyne)$^{+\cdot}$ have quartet ground states as previously discussed [16,39] while Fe(phenyl)$^{+}$ has a quintet ground state. Thus complexes **1**–**3** have the same ground state as

Table 1
Total energies[a] of iron complexes **1**–**3** and fragments

Structure	Spin state	Point group	B3LYP[b] Energy	$\langle S^2 \rangle$	BLYP[c]	ROMP2[c]	PUMP2[c]
1	doublet	C_1	−586.363 429	2.48	−586.109 233	−584.022 117	−584.419 014
	quartet	C_s	−586.399 406	4.71	−586.141 484	−598.516 639	−584.060 306
	sextet	C_{2v}	−586.398 268	8.79	−586.136 008	−584.160 908	−584.132 762
2	doublet	C_{2v}	−586.409 681	1.73	−586.166 673	−584.178 302	−584.196 236
	quartet	C_{2v}	−586.446 489	3.89	−586.194 881	−593.916 179	−584.192 261
	sextet	C_{2v}	−586.368 449	8.76	−586.103 846	−593.708 848	−584.113 011
3	singlet	C_s	−587.043 981	0.00	−586.809 504	−584.761 089[d]	...
	triplet	C_{2v}	−587.040 288	2.68	−586.776 154	−584.728 680	−584.727 309
	quintet	C_{2v}	−587.087 481	6.02	−586.817 582	−584.812 597	−584.811 910
Fe^+(*p*-benzyne)$^{\cdot}$	doublet	C_{2v}	−354.026 920	2.41	−353.903 145	−355.217 459	−352.597 711
	quartet	C_{2v}	−354.081 471	4.65	−353.927 501	−357.091 930	−352.536 375
	sextet	C_{2v}	−354.080 492	8.79	−353.941 096	−357.654 131	−352.601 540
Fe(*o*-benzyne)$^{+\cdot}$	doublet	C_{2v}	−354.091 093	1.71	−353.973 330	−355.117 340	−352.590 830
	quartet	C_{2v}	−354.125 788	3.85	−353.994 008	−352.666 442	−352.650 352
	sextet	C_{2v}	−354.075 888	8.77	−353.943 657	−354.334 695	−352.590 378
Fe(phenyl)$^+$	singlet	C_s	−354.671 428	0.00	−354.538 272	−353.158 687[d]	...
	triplet	C_s	−354.743 361	2.75	−354.598 091	−361.658 819	−353.181 861
	quintet	C_{2v}	−354.770 697	6.03	−354.623 301	−358.981 849	−353.281 547

[a] Energies in hartree.
[b] Fully optimised at this level of theory.
[c] Single-point at B3LYP optimised geometry.
[d] Closed-shell RMP2 value.

their corresponding fragment, which would be generally expected since each complex is simply formed from a neutral closed-shell molecule (benzene) and the fragment.

The results in Table 2 show that **1** and its fragment have low-lying sextet electronic states. Indeed the lowest-lying sextet states are only 3.0 and 2.6 kJ mol^{-1} above the ground states for **1** and its fragment, respectively. This quartet–sextet separation for Fe^+(*p*-benzyne)$^{\cdot}$ may be compared with the value of 20.7 kJ mol^{-1} obtained for this system by Bauschli-

Table 2
Relative energies (kJ mol^{-1}) of spin states of iron complexes **1**–**3** and fragments at B3LYP

Structure	Relative energies		
1	0.0 (quartet)	3.0 (sextet)	94.5 (doublet)
Fe^+(*p*-benzyne)$^{\cdot}$	0.0 (quartet)	2.6 (sextet)	143.2 (doublet)
2	0.0 (quartet)	96.6 (doublet)	204.9 (sextet)
Fe(*o*-benzyne)$^{+\cdot}$	0.0 (quartet)	91.1 (doublet)	131.0 (sextet)
3	0.0 (quintet)	114.2 (singlet)	123.9 (triplet)
Fe(phenyl)$^+$	0.0 (quintet)	71.8 (triplet)	260.6 (singlet)

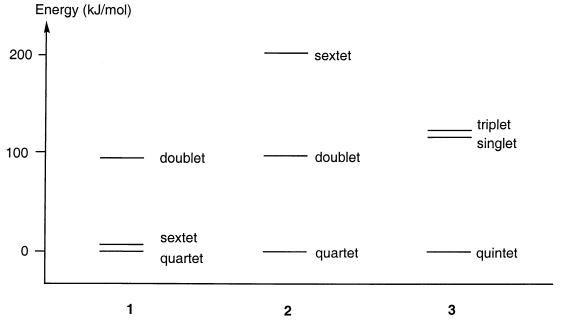

Fig. 1. Relative energies of low lying electronic states of structures **1**–**3** at B3LYP.

cher and co-workers [16] also with the B3LYP method but with an all-electron Wachters basis set on iron [40]. For the other systems considered here there is a larger gap between the ground state and the lowest-lying states of other spin. Fig. 1 shows that there is quite a different pattern in the electronic states for the three complexes. The two excited spin states of **2** are quite spread out while for **3** they lie close together. The fragments show a similar picture to that of Fig. 1, except for Fe(phenyl)$^+$ in which the triplet state lies much lower and the singlet state much higher than in the corresponding complex **3**. This may be a result of the differing geometry between complex and fragment (see the following).

For **1** and its fragment, Fe$^+$(*p*-benzyne)$^{\cdot}$, it makes sense that the quartet and sextet states are so close together since experiments show that the quartet–sextet splitting in Fe$^+$ (24.3 kJ mol^{-1}) [41] and the singlet–triplet splitting in *p*-benzyne (15.9 kJ mol^{-1}) [42] are fairly small. For **2** and its fragment, Fe(*o*-benzyne)$^{+\cdot}$, the quartet state can be understood as arising from the coupling of *o*-benzyne with the ^6D state of Fe$^+$, while the doublet state arises from the coupling of *o*-benzyne with the ^4F state of Fe$^+$, as previously explained [39]. An excellent account of the electrostatic bonding mechanism in Fe(*o*-benzyne)$^{+\cdot}$ versus insertion into the C–C π bond is given in [39]. Since the ^6D state of Fe$^+$ is lower than the ^4F state [41], it also makes sense that for **3** and its fragment, Fe(phenyl)$^+$, the quintet state is lower than the triplet state (although the difference is much larger). What is puzzling at first sight is why the singlet state of **3** is so low in energy. However this can be explained by considering the odd geometry of singlet **3** (see below) which shows that it is not formed from a simple bringing together of benzene, Fe$^+$ and phenyl radical but rather involves some geometrical (and therefore electronic) rearrangement.

A note of caution should be sounded about the spin-state energy differences presented here, because as noted above some of the wave functions suffer from significant spin contamination. However, it has been noted previously (see, e.g. [43] and [44]) that density functional theory is more robust than Hartree-Fock theory with respect to spin contamination. In this sense, BLYP should in principle be better than B3LYP since it incorporates no Hartree-Fock exchange. Single-point energies with BLYP, ROMP2, and PUMP2 bear this out to some extent. Thus the BLYP $\langle S^2 \rangle$ values for the quartet states of **1** and **2** are 4.52 and 3.81, respectively, which are only marginally lower than the B3LYP values of 4.71 and 3.89 (Table 1). However both these sets of values are considerably lower than the PUMP2 $\langle S^2 \rangle$ values for the quartet states of **1** and **2** of 5.53 and 4.91, respectively. The energies obtained with the BLYP method closely parallel the B3LYP energies, with two exceptions. The first is that BLYP stabilises the singlet state of **3** quite significantly compared with the quintet state. The second exception involves the strong stabilisation of the sextet state of Fe$^+$(*p*-benzyne)$^{\cdot}$ at BLYP which leads to it becoming the ground state (by 35.7 kJ mol^{-1}) at this level of theory. The ROMP2 numbers are particularly bad (see, e.g. the ROMP2 total energies of the fragments in Table 1) which could well result from inappropriate reference wave functions (caused by instabilities in the wave functions). From the point of view of calculating excitation energies or complexation energies these numbers are worthless. The spin-projected UMP2 numbers show better agreement with the density functional theory values, except for **1** and Fe$^+$(*p*-benzyne)$^{\cdot}$ where the doublet and sextet states are predicted to lie more than 160 kJ mol^{-1} below the formal quartet ground states. (See also [45] for a discussion of the limitations of UHF-based MP2 methods in the treatment of organometallic systems such as these.) We note in passing that we have not considered open-shell singlets in this work. A more rigorous and balanced treatment of all the various electronic states might be achieved with the use of the complete active space self-consistent field (CASSCF) and complete active space with perturbation theory 2nd order (CASPT2) methods, however it has been noted previously [46] in related work on excited state systems that density functional theory can give reasonable results at far less cost than the multireference methods mentioned above or the time-consuming coupled cluster single double (triple) [CCSD(T)] method. Indeed, B3LYP has been em-

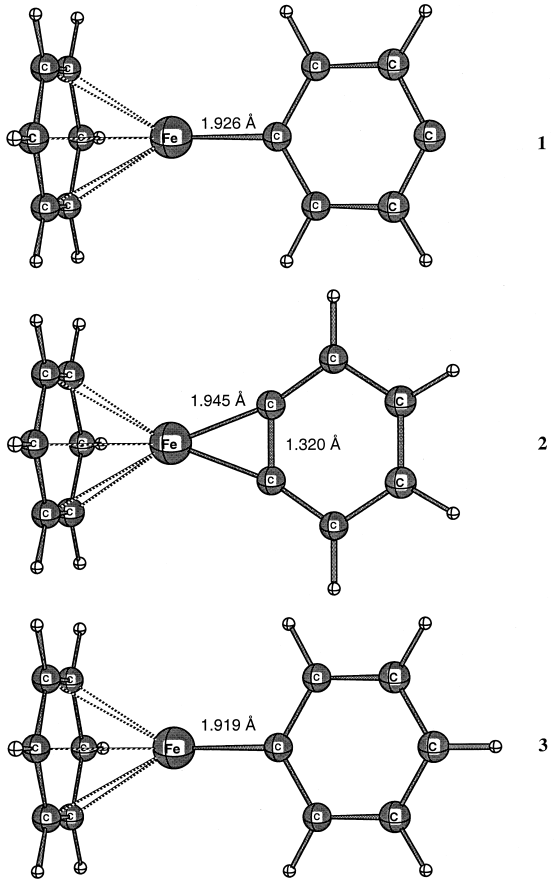

Fig. 2. B3LYP optimised geometries for the ground states of structures **1**–**3**.

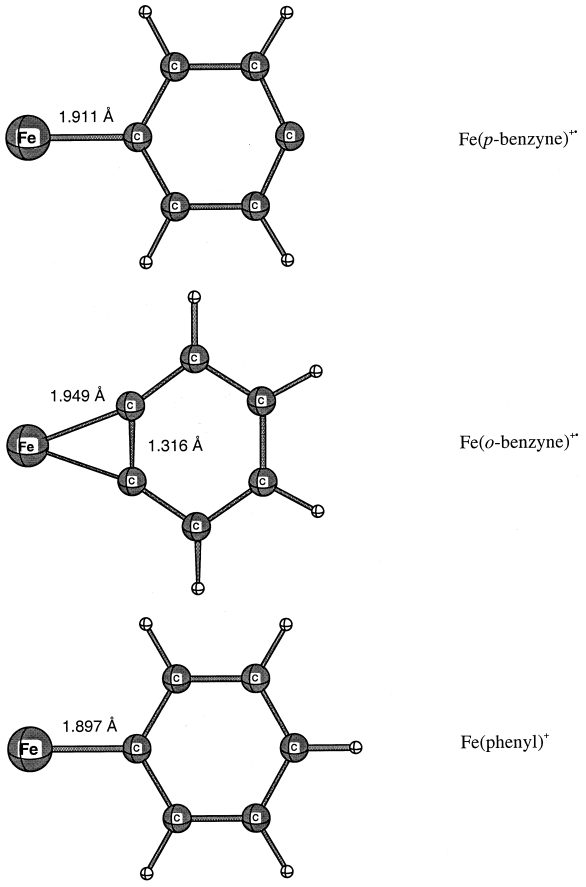

Fig. 3. B3LYP optimised geometries for the ground states of the fragments.

ployed in a number of studies on Fe^+–aryne systems [16,47].

3.2. Geometries

Geometries for the ground states of structures **1**–**3** are shown in Fig. 2 (full details are available in the supporting information). For the most part these are fairly regular structures and correspond to the expected symmetry. The exception is complex **1** which is C_s symmetry, but even this is very close to being a C_{2v} structure. The Fe–C distances are shown in Fig. 2 and the corresponding distances between Fe and the midpoint of the benzene ring are 2.102, 2.074, and 2.111 Å for the ground states of **1**, **2**, and **3**, respectively. Interestingly, the shorter the Fe–C distance, the longer the Fe–ring distance. One simplistic interpretation might be that the shorter Fe–C distances correspond to stronger σ bonds, which occur at the expense of iron's ability to bind to the arene. For comparison, the Fe–ring distance in the ground state of Fe^+–benzene is calculated to be 1.744 Å at the B3LYP/LANL2DZ:6-31G(*d*) level of theory (this work) and 1.830 Å at the MCPF/DZP level [48].

The geometries of the ground states of the corresponding fragments are shown in Fig. 3. These also exhibit very regular C_{2v} structures. Our calculated geometry for Fe(*o*-benzyne)$^{+\cdot}$ may be compared to that obtained previously by Bauschlicher [39] in which the Fe–C distance at the modified coupled pain

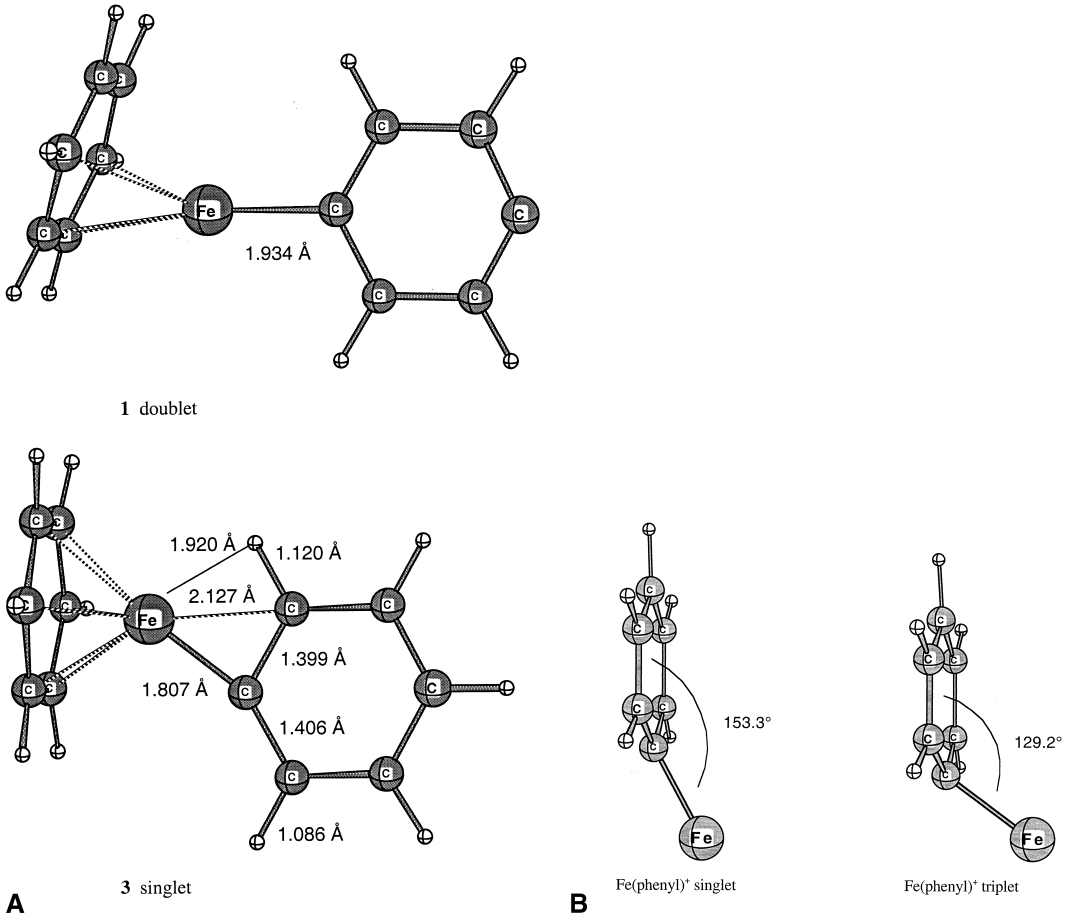

Fig. 4. B3LYP optimised geometries for some unusual structures.

functional (MCPF) level was 1.938 Å and the C–C distance (as shown in Fig. 3) at the CASSCF level was 1.329 Å. Thus our B3LYP values show a slightly weaker binding between iron cation and *o*-benzyne. Comparing the fragments with their complexes it is apparent that the effect of complexation with benzene is to lengthen the Fe–C distances in **1** and **3** and to have little effect in **2**.

The geometries of the lowest-lying electronic states of different spin to the ground state generally have shorter Fe–C distances. The shorter Fe–C distances in sextet **1** (1.918 Å) and sextet Fe^+(*p*-benzyne)$^{\cdot}$ (1.898 Å) may indicate an increase in binding in these excited states at the expense of electron promotion. On the other hand the smaller Fe–C distances in doublet **2** (1.887 Å) and its fragment (1.857 Å) are probably due to the smaller size of the ^4F state of Fe^+ from which these complexes are formed. While many of these excited states have regular C_{2v} structures, a number of unusual structures were found, as shown in Fig. 4. Since these may well be artifacts of the single-reference treatment in this work we will not dwell on them here, but we note that all were obtained by following small imaginary frequencies in the initially optimised C_{2v} structures. The off-centre metal–arene structure in doublet **1** is reminiscent of the slippage effect in metal–alkene complexes [49], while singlet **3** shows not only an unusual metal bridging across C–C–H but also a rather short (1.603 Å) Fe–arene distance.

Table 3
Mulliken charges and spin densities for ground states of iron complexes **1**–**3** and fragments at B3LYP

Structure	Spin state	Charges[a,b]	Spin densities[a]
1	quartet	+0.33 Fe (+1.06 Fe)	2.51 Fe, 0.86 C7, −0.37 C5
Fe^+(*p*-benzyne)$^{\cdot}$	quartet	+0.83 Fe, −0.25 C5 (+0.94 Fe, −0.31 C5)	3.70 Fe, −0.86 C7
2	quartet	+0.33 Fe (+1.06 Fe)	3.11 Fe
Fe(*o*-benzyne)$^{+\cdot}$	quartet	+0.75 Fe (+1.08 Fe)	3.17 Fe
3	quintet	+0.46 Fe, −0.25 C5 (+1.19 Fe, −0.46 C5)	3.65 Fe
Fe(phenyl)$^+$	quintet	+0.84 Fe, −0.27 C5 (+1.11 Fe, −0.39 C5)	3.76 Fe

[a] C5 is the carbon in *p*-benzyne or phenyl to which iron is directly attached, while C7 is the carbon with the formal radical site (i.e. para to the iron).
[b] Numbers in parentheses correspond to the natural charges obtained from a natural population analysis.

3.3. Charge and spin

Mulliken population analyses of the ground-state wave functions lead to the charges and spin densities displayed in Table 3. Structure **1** is found to have $+0.33e$ charge on iron and $0.86e$ spin density on the C_6H_4 carbon atom para to the iron. This may be compared with values of $+0.83e$ charge and $0.86e$ spin density, respectively, for Fe^+(*p*-benzyne)$^{\cdot}$. Thus these are true distonic ions, with their charge and radical sites separated by some 4.6 Å. This is not the case for the other structures studied and as expected **2**, **3** and their corresponding fragments all have both the positive charge and unpaired electrons localised on iron.

"Covering" the iron in the fragments with benzene (to give **1**, **2**, and **3**) leads to a decrease in positive charge on the iron in every case (Table 3). However it may be that this is an artifact of the Mulliken population analyses, since when the calculations were repeated with natural population analyses it was found that the natural charges on iron remain essentially constant (see numbers in parentheses in Table 3). Instead, the reduction in reactivity of the metal centre observed experimentally upon attachment of benzene to the metal [17] may simply be due to the reduced accessibility of the metal. Under the same conditions the reactivity of the radical site is enhanced. This is not borne out by the calculations here which show that the magnitude of the unpaired electron density at the para carbon stays the same on going from Fe^+(*p*-benzyne)$^{\cdot}$ to complex **1**. A careful inspection of Table 3 shows that there are some differences in the electron densities of Fe^+(*p*-benzyne)$^{\cdot}$ and **1**, but more sophisticated calculation and analysis of the wave functions is required to rationalise the experimental result.

3.4. Relative energies

Relative energies for the dissociation of the ground-state complexes to form benzene plus the appropriate fragments are shown in Table 4. At the B3LYP level the dissociation energy of **1** is less than that of **2** but greater than that of **3**. Zero-point vibrational energy corrections to the relative energies are fairly small (5–6 kJ mol^{-1}, see Table 4) and do

Table 4
Ground state dissociation energies of iron complexes **1**–**3**[a]

Structure	Spin state	B3LYP	BLYP	PUMP2
1	quartet	181.9 (175.6)[b]	180.6[c]	173.8
2	quartet	189.2 (183.5)[b]	181.9	221.0
3	quintet	178.9 (174.2)[b]	164.6	190.7

[a] Energy in kJ mol^{-1} for dissociation of complex to form benzene plus appropriate fragment.
[b] Includes zero-point vibrational energy correction.
[c] For dissociation to sextet state of Fe^+(*p*-benzyne)$^{\cdot}$.

not change the relative ordering of the complexes. This relative ordering is maintained at BLYP. [However note that this is based on the ground state of the fragment Fe^+(*p*-benzyne)$^{\cdot}$ which is sextet at the BLYP level rather than quartet (refer back to Table 1)—dissociation of **1** to the quartet state of the fragment is calculated to be 35.7 kJ mol^{-1} higher at the BLYP level.] The PUMP2 dissociation energies are somewhat higher than the density functional ones for **2** and **3**, but lower for **1**. This destabilisation of **1** is probably an artifact of the single-point MP2 method since with this procedure the relative energies of the electronic states of **1** are quite different to the other levels of theory used.

Absolute dissociation energies of these complexes are difficult to measure experimentally, but an estimate of the relative ordering may be obtained from analysis of the energy-resolved collision-induced dissociation plots [17]. On close inspection of Fig. 1 in [17], it appears that the experimental ordering of the dissociation energies is **1** < **3** < **2** (based on the collision energy required to reduce the relative intensity of each complex). Our calculations show that **1** < **2** and that **3** < **2** which agrees with experiment, but that **3** < **1** which does not. Clearly further work at higher levels of theory and with larger basis sets is required to understand this result. One should not attach too much significance to these findings since in studies on the dissociation energies of Fe^+L complexes (with L = O and H_2O) [50,51] it has been shown that B3LYP can easily be in error by 20 kJ mol^{-1} (we emphasise that this applies to dissociation energies—the reliability of geometries and some other properties calculated with B3LYP is usually much better than this).

The dissociation energies of all three complexes are somewhat lower than the corresponding experimental (208 kJ mol^{-1}) [52] or theoretical (215 kJ mol^{-1}) [48] binding energies for Fe^+–benzene. Complex **2** has been studied previously by other experimentalists [53]. The dissociation reaction of **2** to give Fe(*o*-benzyne)$^{+\cdot}$ plus benzene was investigated, but no energetics were reported.

Finally, although it is not the major goal of this work, it is interesting to use the total energies in Table 1 to calculate the relative energies of Fe^+(*p*-benzyne)$^{\cdot}$ and Fe(*o*-benzyne)$^{+\cdot}$. If we restrict ourselves to the quartet states of these species, the para isomer is higher in energy than the ortho isomer by 116.4, 174.6, and 299.2 kJ mol^{-1} at the B3LYP, BLYP, and PUMP2 levels, respectively. Thus there is quite a difference between the three methods, but our B3LYP value is remarkably close to the value of 115.9 kJ mol^{-1} computed by Bauschlicher and co-workers [16] using B3LYP and an all-electron basis set on iron. (Inclusion of zero-point vibrational energies lowers our B3LYP number by 4 kJ mol^{-1}.) These values may be compared with the experimental relative energies of the free benzynes [54] in which *p*-benzyne lies higher in energy than *o*-benzyne by 130.5 kJ mol^{-1}.

4. Concluding remarks

The results presented here show that the positive charge and radical sites are indeed separated for complex **1** and Fe^+(*p*-benzyne)$^{\cdot}$, and that these are true organometallic distonic radical cations. This is in contrast to **2** and **3** which, as expected, show the charge and radical sites localised on the metal. The calculations show that the positive charge on the metal is not really reduced upon complexation with benzene, suggesting that the observed reduction in reactivity may be due more to steric factors. In addition, the radical site in **1** is no more pronounced than in Fe^+(*p*-benzyne)$^{\cdot}$ in contrast to the observed increase in radical reactivity of **1**. Higher level calculations with more flexible basis sets may help to resolve this issue and to obtain better estimates of the relative dissociation energies of the three complexes.

Acknowledgements

This work was supported by the Australian Research Council and the Australian National University Supercomputer Facility.

Supporting information available: The geometries (cartesian coordinates) and zero-point vibrational energies of structures **1**–**3** and their fragments, relative

energies of all spin states at various levels of theory, and Mulliken charges and spin densities for all spin states are listed in the supporting information which may be downloaded from http://www.chem.utas.edu.au/staff/yatesb/fe_distonic.html.

References

[1] B.F. Yates, W.J. Bouma, L. Radom, J. Am. Chem. Soc. 106 (1984) 5805.
[2] L. Radom, W.J. Bouma, R.H. Nobes, B.F. Yates, Pure Appl. Chem. 56 (1984) 1831.
[3] B.F. Yates, W.J. Bouma, L. Radom, Tetrahedron 42 (1986) 6225.
[4] S. Hammerum, Mass Spectrom. Rev. 7 (1988) 123.
[5] K.M. Stirk, L.K.M. Kiminkinen, H.I. Kenttämaa, Chem. Rev. 92 (1992) 1649.
[6] B.T. Hill, J.C. Poutsma, L.J. Chyall, J. Hu, R.R. Squires, J. Am. Soc. Mass Spectrom. 10 (1999) 896.
[7] K. Pius, J. Chandrasekhar, J. Chem. Soc., Perkin Trans. 2 (1988) 1291.
[8] Y. Guo, J.J. Grabowski, J. Am. Chem. Soc. 113 (1991) 5923.
[9] J. Kauw, M. Born, S. Ingemann, N.M.M. Nibbering, Rapid Commun. Mass Spectrom. 10 (1996) 1400.
[10] J.J. Nash, R.R. Squires, J. Am. Chem. Soc. 118 (1996) 11872.
[11] M. Born, S. Ingemann, N.M.M. Nibbering, Mass Spectrom. Rev. 16 (1997) 181.
[12] P.G. Wenthold, J. Hu, B.T. Hill, R.R. Squires, Int. J. Mass Spectrom. 180 (1998) 173.
[13] J. Hu, R.R. Squires, J. Am. Chem. Soc. 118 (1996) 5816.
[14] K.K. Thoen, H.I. Kenttämaa, J. Am. Chem. Soc. 119 (1997) 3832.
[15] J. Hu, B.T. Hill, R.R. Squires, J. Am. Chem. Soc. 119 (1997) 11699.
[16] Y.C. Xu, S.A. Lee, B.S. Reiser, C.W. Bauschlicher, J. Am. Chem. Soc. 117 (1995) 5413.
[17] Y.C. Xu, Q. Chen, S.K. Poehlein, B.S. Freiser, Rapid Commun. Mass Spectrom. 13 (1999) 645.
[18] K.M. Stirk, J.C. Orlowski, D.T. Leeck, H.I. Kenttämaa, J. Am. Chem. Soc. 114 (1992) 8604.
[19] H.I. Kenttämaa, Org. Mass Spectrom. 29 (1994) 1.
[20] A.D. Becke, J. Chem. Phys. 98 (1993) 5648.
[21] P.J. Stephens, J.F. Devlin, C.F. Chabalowski, M.J. Frisch, J. Phys. Chem. 98 (1994) 11623.
[22] R.H. Hertwig, W. Koch, Chem. Phys. Lett. 268 (1997) 345.
[23] P.J. Hay, W.R. Wadt, J. Chem. Phys. 82 (1985) 299.
[24] W.J. Hehre, R. Ditchfield, J.A. Pople, J. Chem. Phys. 56 (1972) 2257.
[25] P.C. Hariharan, J.A. Pople, Chem. Phys. Lett. 16 (1972) 217.
[26] R. Seeger, J.A. Pople, J. Chem. Phys. 66 (1977) 3045.
[27] R. Bauernschmitt, R. Ahlrichs, J. Chem. Phys. 104 (1996) 9047.
[28] G.B. Bacskay, Chem. Phys. 61 (1981) 385.
[29] A.D. Becke, J. Chem. Phys. 88 (1988) 1053.
[30] C. Lee, W. Yang, R.G. Parr, Phys. Rev. B 37 (1988) 785.
[31] B. Miehlich, A. Savin, H. Stoll, H. Preuss, Chem. Phys. Lett. 157 (1989) 200.
[32] C. Møller, M.S. Plesset, Phys. Rev. 46 (1934) 618.
[33] J.A. Pople, J.S. Binkley, R. Seeger, Int. J. Quantum Chem., Symp. 10 (1976) 1.
[34] M. Head-Gordon, J.A. Pople, M.J. Frisch, Chem. Phys. Lett. 153 (1988) 503.
[35] R.D. Amos, J.S. Andrews, N.C. Handy, P.J. Knowles, Chem. Phys. Lett. 185 (1991) 256.
[36] H.B. Schlegel, J. Chem. Phys. 84 (1986) 4530.
[37] M.J. Frisch, G.W. Trucks, H.B. Schlegel, P.M.W. Gill, B.G. Johnson, M.A. Robb, J.R. Cheeseman, T. Keith, G.A. Petersson, J.A. Montgomery, K. Raghavachari, M.A. Al-Laham, V.G. Zakrzewski, J.V. Ortiz, J.B. Foresman, J. Cioslowski, B.B. Stefanov, A. Nanayakkara, M. Challacombe, C.Y. Peng, P.Y. Ayala, W. Chen, M.W. Wong, J.L. Andres, E.S. Replogle, R. Gomperts, R.L. Martin, D.J. Fox, J.S. Binkley, D.J. Defrees, J. Baker, J.P. Stewart, M. Head-Gordon, C. Gonzalez, J.A. Pople, GAUSSIAN 94, Revision C.2, Gaussian, Inc., Pittsburgh, PA, 1995.
[38] M.J. Frisch, G.W. Trucks, H.B. Schlegel, G.E. Scuseria, M.A. Robb, J.R. Cheeseman, V.G. Zakrzewski, J.A. Montgomery, R.E. Stratmann, J.C. Burant, S. Dapprich, J.M. Millam, A.D. Daniels, K.N. Kudin, M.C. Strain; O. Farkas, J. Tomasi, V. Barone, M. Cossi, R. Cammi, B. Mennucci, C. Pomelli, C. Adamo, S. Clifford, J. Otcherski, G.A. Petersson, P.J. Ayala, Q. Cui, K. Morokuma, D.K. Malick, A.D. Rabuk, K. Raghavachari, J.B. Foresman, J. Cioslowski, J.V. Ortiz, B.B. Stefanov, G. Liu, A. Liashenko, P. Piskorz, I. Komaromi, R. Gomberts, R.L. Martin, D.J. Fox, T. Kieth, M.A. Al-Laham, C.Y. Peng, A. Nanayakkara, C. Gonzalez, M. Challacombe, P.M.W. Gill, B.G. Johnson, W. Chen, M.W. Wong, J.L. Andres, M. Head-Gordon, E.S. Replogle, J.A. Pople, GAUSSIAN 98, Revision A.1; Gaussian, Inc., Pittsburgh, PA, 1998.
[39] C.W. Bauschlicher, J. Phys. Chem. 97 (1993) 3709.
[40] C.W. Bauschlicher, personal communication.
[41] C.E. Moore, Atomic Energy Levels; U.S. National Bureau of Standards (U.S.) Circular No. 467, U.S. Bureau of Standards, Washington, DC, 1949.
[42] P.G. Wenthold, R.R. Squires, W.C. Lineberger, J. Am. Chem. Soc. 120 (1998) 5279.
[43] J.A. Pople, P.M.W. Gill, N.C. Handy, Int. J. Quantum. Chem. 56 (1995) 303.
[44] J.M. Wittbrodt, H.B. Schlegel, J. Chem. Phys. 105 (1996) 6574.
[45] P. Taylor, in Lecture Notes in Quantum Chemistry, B.O. Roos, (Ed.), Springer, Heidelberg, 1992.
[46] P.R. Schreiner, J. Am. Chem. Soc. 120 (1998) 4184.
[47] H. Chen, D.B. Jacobson, B.S. Freiser, Organometallics 18 (1999) 1774.
[48] C.W. Bauschlicher, H. Partridge, S.R. Langhoff, J. Phys. Chem. 96 (1992) 3273.
[49] O. Eisenstein, R. Hoffmann, J. Am. Chem. Soc. 102 (1980) 6149.
[50] M. Filatov, S. Shaik, Chem. Phys. Lett. 288 (1998) 689.
[51] A. Irigoras, J.E. Fowler, J.M. Ugalde, J. Am. Chem. Soc. 121 (1999) 8549.
[52] F. Meyer, F.A. Khan, P.B. Armentrout, J. Am. Chem. Soc. 117 (1995) 9740.
[53] Y. Huang, D.R.A. Ranatunga, B.S. Freiser, J. Am. Chem. Soc. 116 (1994) 4796.
[54] P.G. Wenthold, R.R. Squires, J. Am. Chem. Soc. 116 (1994) 6401.